Dalton Transactions

Accepted Manuscript

This article can be cited before page numbers have been issued, to do this please use: T. Morais, Y. Jousseaume, M. F. Minas da Piedade, C. Rodrigues, A. Fernandes, F. M. Marques, M. V. Brito and M. H. Garcia, *Dalton Trans.*, 2018, DOI: 10.1039/C8DT01653D.

This is an Accepted Manuscript, which has been through the Royal Society of Chemistry peer review process and has been accepted for publication.

Accepted Manuscripts are published online shortly after acceptance, before technical editing, formatting and proof reading. Using this free service, authors can make their results available to the community, in citable form, before we publish the edited article. We will replace this Accepted Manuscript with the edited and formatted Advance Article as soon as it is available.

You can find more information about Accepted Manuscripts in the author guidelines.

Please note that technical editing may introduce minor changes to the text and/or graphics, which may alter content. The journal's standard Terms & Conditions and the ethical guidelines, outlined in our author and reviewer resource centre, still apply. In no event shall the Royal Society of Chemistry be held responsible for any errors or omissions in this Accepted Manuscript or any consequences arising from the use of any information it contains.

ROYAL SOCIETY OF CHEMISTRY

rsc.li/dalton

ROYAL SOCIETY OF CHEMISTRY View Article Online
DOI: 10.1039/C8DT01653D

Journal Name

ARTICLE

Important cytotoxic and cytostatic effects of new Copper(I)-phosphane compounds with NN, NO and NS bidentate ligands

Received 00th January 20xx,
Accepted 00th January 20xx

DOI: 10.1039/x0xx00000x

www.rsc.org/

Tânia S. Morais*[a,b], Yann Jousseaume[a,b], M. Fátima M. Piedade[b,c], Catarina Roma-Rodrigues[d], Alexandra R. Fernandes[d], Fernanda Marques[e], Maria J. Villa de Brito*[a,b], M. Helena Garcia[a,b]

A family of six phosphane Cu(I) complexes bearing NN, NO and NS bidentate ligands was synthesized. All the compounds were fully characterized by classical analytical and spectroscopic methods and five of them were also characterized by X-ray diffraction studies. All the compounds exhibit high cytotoxicity against the human breast cancer cell line MCF7 with IC_{50} values far lower than those found for cisplatin, a current chemotherapeutic in clinical use. Compounds **1** and **3** induce cell cycle arrest in G2/M phase and cell death by apoptosis. The cytotoxic and cytostatic effect of these compounds on MCF7 cells suggest that they are suitable for further *in vivo* studies with breast cancer models.

Introduction

Copper is an essential micronutrient involved in fundamental life processes. It readily cycles between Cu(I) and Cu(II), which makes it redox active in biological systems. This redox-cycling ability is vital for cooper to act as a key component of many important metalloenzymes and metalloproteins with important roles in biological functions such as enzyme activity, cell signalling and oxygen transport[1-3].

Copper has been recognized as a controlling factor for a variety of processes related to cancer development and progression, particularly in cancer growth, angiogenesis and metastasis[4, 5].

Elevated levels of copper and oxidative stress have been found in cancer conditions, thus providing an opportunity to exploit these differences for the development of cancer treatment strategies[6]. Additionally, altered copper metabolism can also constitute a promising target for cancer therapy[7].

The vast array of information on copper properties and mode of action in several biological systems, together with the assumption that endogenous metals may be less toxic, led to the development of a novel generation of copper coordination compounds for cancer therapy with properties generally determined by the nature of ligands and donor atoms bound to the metal ion[8-10]. In this frame, several classes of copper complexes containing phosphanes, imidazoles, thiosemicarbazones and carbenes have been identified as potential anticancer agents[8, 11-17].

Some of these promising copper complexes can be effective anticancer agents as much as platinum-based drugs, with the advantage of reduced toxicity toward normal cells and can even potentially overcome resistance associated with platinum drugs. For this particular process of chemoresistance, copper transporters play a central role. Certain copper coordination compounds can modulate the copper homeostasis across the copper transporters and hence re-sensitize cancer cells to platinum drugs [8, 18-20].

Despite the different classes of copper coordination compounds synthesized and characterized, few data are available concerning the mechanisms underlying their anticancer activity. Nevertheless, the reported data suggest that copper compounds display mechanisms of action mainly based on the ability to induce apoptosis, oxidative stress, inhibition of proteasome activity and non-apoptotic forms of programmed cell death[6, 21-25]

In the scope of copper coordination compounds we recently reported our studies on a family of copper(I)-phosphane complexes of general formula $[Cu(dppe)L][BF_4]$, where dppe = 1.2-bis(diphenylphosphino)ethane and L represents a bidentate heteroaromatic ligand with N-donor atoms. These complexes bearing dppe phosphane ligands showed marked cytotoxic activity against A2780 and MCF7 cancer cells at submicromolar concentrations [26].

Our ongoing research interest on this field led us to keep on the exploitation of related copper(I) compounds in a systematic fashion, focusing on the design and synthesis of new complexes involving coordination of various ligands to a similar metal-phosphane fragment so as to assess the effect of individual structural changes on the cytotoxic properties of the compounds. Thus, in this paper we

[a] Centro de Química Estrutural, Faculdade de Ciências, Universidade de Lisboa, Portugal.
[b] Departamento de Química e Bioquímica, Faculdade de Ciências, Universidade de Lisboa, Portugal
[c] Centro de Química Estrutural, Instituto Superior Técnico, Universidade de Lisboa, Portugal
[d] UCBIO, Departamento de Ciências da Vida, Faculdade de Ciências e Tecnologia, Universidade Nova de Lisboa, Portugal
[e] Centro de Ciências e Tecnologias Nucleares, Instituto Superior Técnico, Universidade de Lisboa, Portugal
E-mail: tsmorais@ciencias.ulisboa.pt (T.S. Morais); mjbrito@ciencias.ulisboa.pt (M.J. Villa de Brito)
† Footnotes relating to the title and/or authors should appear here.
Electronic Supplementary Information (ESI) available: [details of any supplementary information available should be included here]. See DOI: 10.1039/x0xx00000x

View Article Online
DOI: 10.1039/C8DT01653D

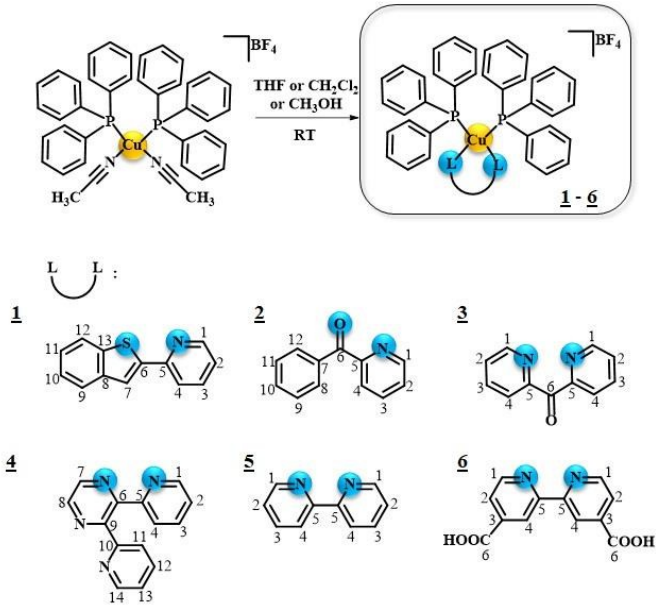

Scheme 1 Reaction scheme for the synthesis of the $[Cu(PPh_3)_2(L)][BF_4]$ compounds (L= pbt, **1**; bopy, **2**; dpk, **3**; dpp, **4**; 2,2'bipy, **5** and dcbipy, **6**). Ligands are numbered for NMR spectral assignments.

report the synthesis and characterization of new Cu(I) complexes of general formula $[Cu(PPh_3)_2L][BF_4]$ where L represents different NN, NO or NS bidentate systems. The cytotoxic activity, the ability to induce apoptosis and cell cycle arrest was also evaluated in MCF7 breast human cell line.

Results and discussion

Synthesis and Characterization of Cu(I) compounds

Six new Cu(I) complexes of general formula $[Cu(PPh_3)_2(L)][BF_4]$ were prepared in high yields (82-92 %), through substitution of the labile acetonitrile ligands on the parent complex $[Cu(PPh_3)_2(NCMe)_2][BF_4]$ by bidentate ligands L, namely 2-(2-pyridyl)benzo[b]thiophene (pbt), **1**, 2- benzoylpyridine (bopy), **2**, di(2-pyridyl)ketone (dpk), **3**, 2,3-bis(2-pyridyl)pyrazine (dpp), **4**, 2,2'-bipyridine (2,2'-bipy), **5** and 2,2'-bipyridine-4,4'-dicarboxylic acid (dcbipy), **6**. The reactions were carried out in THF, dichloromethane or methanol solutions at room temperature (**Scheme 1**). The compounds were recrystallized, at room temperature, by slow diffusion of diethyl ether in dichloromethane solutions of the compounds.

The new complexes were fully characterized by FTIR and NMR spectroscopic methods (^1H, $^{13}C\{^1H\}$, $^{31}P\{^1H\}$). The elemental analyses were in accordance with the proposed formulations. Compounds **1**, **2**, **3**, **4** and **5** were also characterized by single crystal X-ray diffraction techniques. The FTIR spectra of all the compounds in KBr pellets present the characteristic ν_{C-H} bands of aromatic rings in the region 3040 – 3100 cm^{-1}, the $\nu_{C=C}$ vibrations appear at 1400 – 1590 cm^{-1} and the δ_{C-H} vibrations in the 690 - 700 cm^{-1} range. The ν_{B-F} vibrations of the BF_4^- anion were observed at 1095-1057 cm^{-1} (very strong and broad bands) and ~690 cm^{-1}. Compounds **2**, **3** and **6** also presented the $\nu_{C=O}$ vibrations in the range 1626 – 1720 cm^{-1} as expected.

NMR Spectroscopic studies

NMR characterization of all complexes was carried out by recording ^1H, $^{13}C\{^1H\}$, $^{31}P\{^1H\}$ and 2D experiments (COSY, HSQC and HMBC). The ^1H and ^{13}C NMR spectra of complexes **1**-**3** and **5** and **6** in acetone-*d*6 or $CDCl_3$ at room temperature displayed well resolved resonances which were fully assigned (see Experimental section and atom labelling given in **Scheme 1**) using those 2D methods.

In contrast, the ^1H NMR signals of complex **4** were very broad in the dpp domain at room temperature. This observation is in accordance with our previous results which showed that the dpp ligand, (2,3-bis(2,3-pyridyl)pyrazine), is quite flexible when coordinated to copper(I), even if the other N,N moiety is chelated to a second metal fragment such as $\{RuCp(PPh_3)\}$[26] and prompted us to undertake a VT-NMR study of this compound to assess its fluxional behavior. The effect of cooling an acetone-d^6 solution of **4** is shown in **Figure S1** in Supplementary Information. As the temperature was lowered, the dpp region in the ^1H NMR spectra became more resolved, showing that one conformer was dominant. The set of 1D and 2D experiments performed at -50ºC permitted full assignment of the ^1H and ^{13}C resonances of the major conformer (see Experimental section). A second set of signals was also detected, with much lower intensity than the dominant peaks (~0.08:1.0), indicating that one conformation is clearly favored for this compound. Evidence of the presence of two conformers in similar ratio proportions, detected by VT-NMR studies of Cu(I) complexes with flexible ligands, has already been reported[26, 27].

The well-defined proton signals observed for all the compounds also confirm that no oxidation to Cu(II) occurred under the experimental conditions.

The $^{31}P\{^1H\}$ spectra of the new Cu(I) complexes show the usual broad signal ($\nu_{1/2}$= 26–330 Hz) in the range 3.0 – 1.1 ppm, downfield from the parent compound $[Cu(PPh_3)_2(NCMe)_2][BF_4]$, ($\delta$ -0.9 ppm) reflecting a decrease of electron density in the phosphorus atoms as the NCMe ligands are replaced by better acceptor ones.

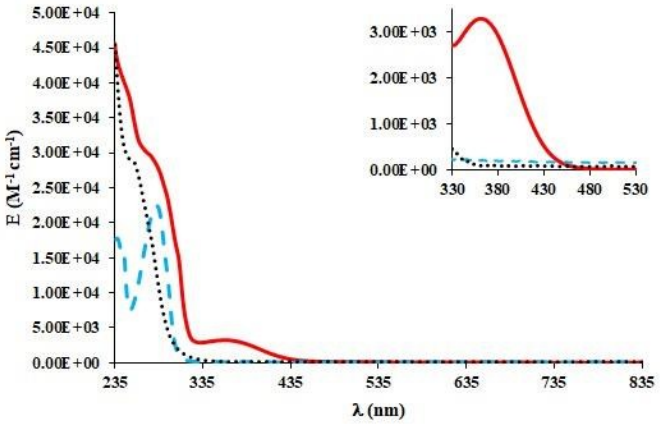

Figure 1 Electronic spectra of $[Cu(PPh_3)_2(2,2'\text{-bipy})][BF_4]$ (**5**) (—), in dichloromethane, compared to the uncoordinated ligand 2,2'-bipyridine (– – –) and $[Cu(PPh_3)_2(NCMe)_2][BF_4]$ (· · · ·). Inset: detail of the charge transfer band.

View Article Online
DOI: 10.1039/C8DT01653D

Table 1 Electronic spectra data for complexes **1** – **6**, precursor and free ligands, in dichloromethane solutions.

Compound	λmax (nm) (ε $M^{-1}cm^{-1}$)	Compound	λmax (nm) (ε $M^{-1}cm^{-1}$)
$[Cu(PPh_3)_2(NCMe)_2][BF_4]$	259 (sh)		
	279 (sh)		
$[Cu(PPh_3)_2(pbt)][BF_4]$ (**1**)	258 (sh)	pbt	–
	279 (sh)		262 (sh)
	319 (22200)		315 (40200)
	333 (sh)		328 (sh)
$[Cu(PPh_3)_2(bopy)][BF_4]$ (**2**)	272 (38800)	bopy	266 (14300)
	417 (3300)		354 (225)
$[Cu(PPh_3)_2(dpk)][BF_4]$ (**3**)	–	dpk	244 (11900)
	270 (35000)		277 (11200)
	426 (2120)		360 (206)
$[Cu(PPh_3)_2(dpp)][BF_4]$ (**4**)	265 (30700)	dpp	252 (20900)
	326 (sh)		288 (27900)
	385 (3310)		–
$[Cu(PPh_3)_2(2,2'\text{-bipy})][BF_4]$ (**5**)	283 (sh)	2,2'-bipy	244 (15730)
	367 (3310)		282 (22104)
$[Cu(PPh_3)_2(dcbipy)][BF_4]$ (**6**)	256 (sh)	dcbipy	insoluble
	311 (9100)		
	405 (2810)		

These ^{31}P resonances are similar to previously reported values for other Cu(I)-(PPh_3) complexes[17], and show a slight shift to higher frequencies relatively to the Cu(I) dppe analogues that we previously reported[26].

Electronic absorption spectroscopy

The electronic absorption spectra of the six new synthesized copper complexes were recorded in ~10^{-4} to 10^{-6} M solutions of dichloromethane and the corresponding maximum absorption bands are indicated in **Table 1**. For comparison, also the electronic spectra of the free ligands were obtained in the same experimental conditions.

All the studied Cu(I) complexes showed intense absorption bands in the UV region, in the range of 230 – 330 nm, attributed to π-π* electronic transitions occurring in the coordinated ligands of the inorganic fragment $\{Cu(PPh_3)_2\}^+$. In addition to these transitions, one metal to ligand charge transfer (MLCT) band was found, for complexes **2** - **6**, placed in the visible region between 360 and 430 nm. These high values of energy found for MLCT bands were also observed in other Cu(I) compounds with dppe and N,N heteroaromatic rings[26]. The absorption spectra found for compound **5** is in agreement with those published by Andrés-Tomé *et al.* for the same compound[28]. **Figure 1** typifies the behavior of this set of compounds.

Stability studies in DMSO and DMSO/DMEM

The stability of the complexes in DMSO-*d6* (deuterated form of the co-solvent used in the biological assays) was studied by ^1H and ^{31}P NMR spectroscopy over 24 h. In both, ^1H and ^{31}P NMR spectra, no changes were observed either on the number of peaks displayed or on their δ values (**Figure S2** in Supplementary Information).

The stability of the new complexes in 1%DMSO/DMEM + GlutaMAX-I™ cellular medium was also evaluated by UV–vis spectroscopy. Changes observed in UV–vis spectrum of the complexes over 24 h were insignificant, indicating that these complexes are air-stable in this solution (**Figure S3** in Supplementary Information).

Crystal structures of complexes 1,2, 3, 4 and 5

Single crystals of complexes **1**, **2**, **3**, **4** and **5** suitable for SCXRD were obtained by slow diffusion of diethyl ether in dichloromethane solution of the corresponding complexes. The X-ray single crystal data of all compounds were analyzed in the temperature range 160 – 150 K to prevent disorder of the molecules. The molecular structures of the compounds are presented in **Figure 2** and selected bond lengths and angles are displayed in **Table 2**.

The five compounds crystallize in triclinic crystal system, space group P -1, with a cationic complex molecule and a BF_4 as a counter anion in the asymmetric unit; complex **2** co-crystalizes with CH_2Cl_2. The copper(I) ion presents two coordinated triphenylphosphanes and the bidentate ligand L in a highly distorted tetrahedral geometry. This distortion arises from the "bite" of the bidentate ligand, N(1)-Cu(1)-S(1) 77.76(5)° for **1**, N(1)-Cu(1)-O(1) 76.55(9)° in **2** and N(1)-Cu(1)-N(2) 92.17(11)°, 79.18(15)°, 79.64(9)° for **3**, **4** and **5** respectively, much smaller than the angle of the perfect tetrahedron, 109.4°. However, the bite angle of the dpk ligand, in compound **3**, is larger than the others as it forms a six-membered ring with the metal center while the others form a five membered metallacycle. Also the P(1)-Cu(1)-P(2) angles (129.37(2)°, 125.96(4)°, 123.14(3)°, 123.76(5)° and 124.91(3)°), for complexes **1**, **2**, **3**, **4**, and **5**, respectively) are larger due to the steric effects caused by the bulky PPh_3 ligands.

View Article Online
DOI: 10.1039/C8DT01653D

Table 2 Selected Bonds (Å) and Bonds Angles (°) of the cations $[Cu(PPh_3)_2(L)]^+$ (L= pbt, **1**; bopy, **2**; dpk, **3**; dpp, **4**; 2,2'bipy, **5**).

Compound	1	2	3	4	5
Bond lengths (Å)					
Cu(1) – N(1)	2.0303(17)	2.050(3)	2.076(3)	2.078(4)	2.099(2)
Cu(1) – X	2.6902(6)	2.211(2)	2.099(3)	2.104(4)	2.055(2)
Cu(1) – P(1)	2.2507(6)	2.2423(11)	2.2796(9)	2.2474(14)	2.2569(8)
Cu(1) – P(2)	2.2509(6)	2.2442(11)	2.2836(9)	2.2459(14)	2.2593(7)
Angles (°)					
X – Cu(1) – N(1)	77.76(5)	76.55(9)	92.17(11)	79.18(15)	79.64(9)
P(2) – Cu(1) – P(1)	129.37(2)	125.96(4)	123.14(3)	123.76(5)	124.91(3)
N(1) – Cu(1) – P(1)	116.39(5)	116.53(8)	115.06(8)	117.33(12)	113.19(6)
N(1) – Cu(1) – P(2)	113.17(5)	112.17(8)	103.38(8)	109.34(12)	107.90(6)
P(1) – Cu(1) – X	106.55(2)	105.06(7)	105.53(8)	104.33(11)	109.64(7)
P(2) – Cu(1) – X	93.08(2)	107.66(6)	113.43(8)	113.93(11)	112.53(6)

Nevertheless these angles along with the bond lengths involving the copper atom are in the range of values found for this family of cations $[Cu(I)(PPh_3)_2L]^+$ (where L is a bidentate ligand)[20, 21]. The pbt ligand in complex **1**, is not planar; the plane of the pyridyl ring and the plane of the benzothiophenyl rings form an angle of 28°, while the free ligand is almost planar with an angle of 7.7°[29]. In compound **2**, the non-planarity of the bidentante ligand is caused by distortion of the phenyl ring attached to the O=C bond making an angle of 47.3° between the two rings, while in the free ligand the same dihedral ligand is much larger, *ca* 61°. This is due to complexation of the ligand to the copper that restrains stereochemically the ligand. The two six membered rings in the bidentate ligand of compound **3** make an angle of 17° and the carbonyl group that binds the two rings is almost coplanar with the ring that contains the N1 atom. In this case, the angle between the two rings is much smaller than the one in the free ligand (55.8°). The cation of complex **4** also presents a non-planar bidentate ligand (dpp) bonded to the copper center. In this ligand, the planes of the rings linked by the C5-C6 bond have an angle of 35.9°, and the planes of the two pyridyl rings make an angle of 44°. The non-planarity of the ligand in the cation of complex **4** is slightly smaller than that in the free ligand were the dihedral angles between the three rings are all equal with a value of 42.2°. However, in the cation of the similar complex with a bidentate phosphine, $[Cu(dppe)(dpp)]BF_4$[26], the dihedral angles between the planes of the rings joined by C5-C6 bond are even smaller (24.8°) and the mean plane of the two rings joined by C5-C6 bond with the aromatic ring that is linked by C9-C10 bond form an angle of 59.8°. In complex **5**, the angle between the rings of the bidentate ligand is *ca.* 17°, although in the free ligand the two rings are totally coplanar. This difference in the angles between the two planes of the N,N coordinated ligand and the one of the free ligands is due to the stereochemical restraint imposed by the two bulky phosphines coordinated to metal centre. The structure of this cation with the $[NO_2]^-$ anion was already described by Navarro *et al.*[30], no significant differences being observed in the bond lengths and angles of the complexes with the two counter-ions.

In the packing of these compounds, the intermolecular interactions found are of the type C-H···F and C-H···π. Compounds **2**, **3** and **4** form chains of cations through C-H···π interactions between phenyl – phenyl rings of the phosphines and phenyl and pyridyl of the bidentate ligand (C-H···π range of 3.1 – 3.5 Å). These cations are also surrounded by 3, 5 and 5 anions, respectively, that form interactions C-H···F ranging from 2.4 Å in compound **4** to 2.9 Å in compound **3**. Compound **3** has an additional interaction of the type C-H···O (2.6 Å) between the carbonyl group and a phenyl of the phosphine.

Each cation of compound **1** has five other cations and five BF_4^- anions in its environment. The cations interact with each other via C-H···π interactions (3.2 Å) between two bidentate ligands and among a bidentate ligand and a phenyl group of the phosphine. A C-H···π interaction between two phenyl rings of the phosphine (3.1 Å) has also been detected.

The anions of **1** display C-H···F interactions with the cations with intermolecular distances in the range of 2.4 to 2.6 Å.

The packing of compound **5** comprises one cation surrounded by 4 other cations and 5 anions. C-H···π interactions are evident between a pyridyl ring of the bidentate ligand and a phenyl ring of PPh_3 and also between two phenyl rings of the phosphines (3.2 and 3.4 Å). The interactions of the cations with the anions (C-H···F) are in the range of 2.4 to 2.6 Å.

Compounds **1** and **5** had a more planar ligand than the other three compounds, leading to a more freely stereochemical environment around the cation, assembling more molecules around each other.

View Article Online
DOI: 10.1039/C8DT01653D

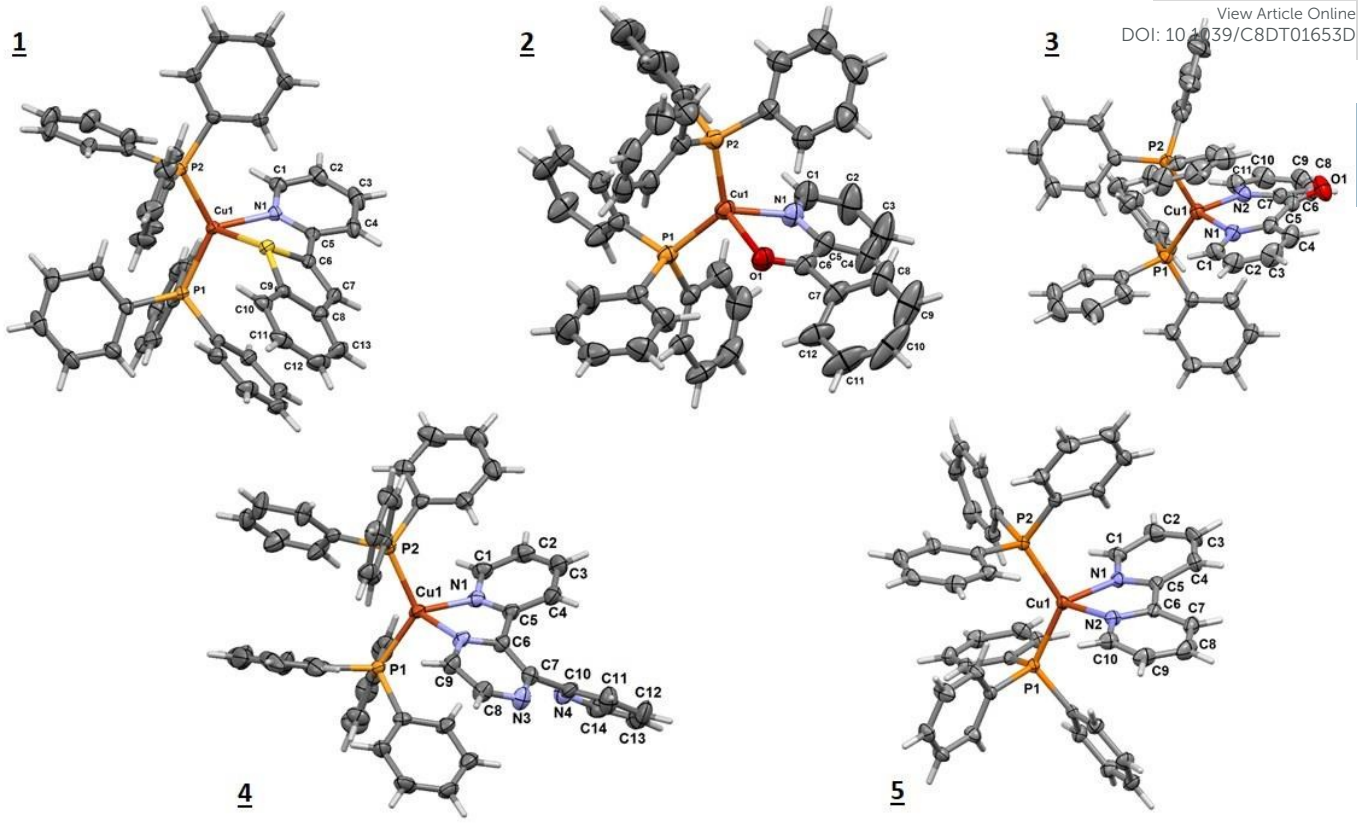

Figure 2 Molecular diagrams depicting the cationic moieties for $[Cu(PPh_3)_2(L)]^+$ complexes (L= pbt, **1**; bopy, **2**; dpk, **3**; dpp, **4**; 2,2'bipy, **5**). Hydrogen atoms were omitted for clarity.

Biological studies in human tumor cells

Cytotoxicity

The cytotoxic potential of compounds **1** - **6** and their precursor in MCF7 adenocarcinoma cells lines was evaluated by the MTT assay to assess cell viability and survival. As observed in **Table 3** all complexes including the precursor $[Cu(PPh_3)_2(NCMe)_2][BF_4]$ are active in the breast adenocarcinoma cancer cells at 24h incubation with IC_{50} values varying from 6.6 to 18 µM.

The activity of the free ligands was also evaluated using the same experimental conditions in MCF7 cells at 24 h incubation. Within the concentration range of 1 - 200 µM the free ligands were not active with the exception of pbt that displayed an IC_{50} value of 55 ± 7.7 µM. The cytotoxic effect of the triphenylphosphane (PPh_3) was also assessed and found negligible. With exception of complexes **1**, **3** and **5** the substitution of the acetonitrile ligands on the parent complex by the bidentate ligands did not result in any considerable improvement of activity. Comparing compounds **5** and **6** the introduction of two carboxylic groups in the 2,2'-bipy ligand resulted in a less active compound. This difference in the activity could be related to the fact that in solution compound **6** has a double negative charge in the carboxylic groups which could hinder the cellular uptake[31]. With the same experimental conditions, all the compounds are much more active than cisplatin, the antitumor drug in clinical use. The IC_{50} values found for the compounds here presented are of the same magnitude order as those found for other copper(I)-triphenylphosphane complexes with heteroaromatic ligands for the same cells[17, 32].

Since the free ligands did not show cytotoxic effect it is possible to conclude that the cytotoxicity of these complexes was in part due to the coordinated triphenylphosphine coligands. Despite this, by substituting the phosphane fragment PPh_3 by dppe in this complexes, as we previously reported, a remarkable improvement of about ten times in the cytotoxic activity was found[26].

Apoptosis evaluation

To understand if the decrease of MCF7 tumor cells viability in the presence of the compounds is due to the induction of apoptosis, cells were treated with the IC_{50} concentration (**Table 3**) of the precursor, compounds **1**, **3** and **5** and respective solvent (DMSO) as vehicle control and DNA staining with Hoechst 33258 was accessed via fluorescence microscopy. Compounds **1**, **3** and **5** were chosen due to their lower relative IC_{50} in MCF7 cells compared to the precursor and compounds **2** and **4**. Staining the cell nuclear DNA with Hoechst allows to infer the presence of apoptotic events, including condensation of the chromatin, fragmentation of the nucleus and the presence of the so called apoptotic vesicle[33]. Hoechst staining revealed an increased number of nucleus with condensed chromatin

Table 3 IC_{50} values found for compounds (**1** – **6**), precursor and cisplatin in the breast adenocarcinoma MCF7 cells (24 h, 37 °C).

Compound	IC_{50} (μM)
$[Cu(PPh_3)_2(NCMe)_2][BF_4]$	13.4 ± 5.3
$[Cu(PPh_3)_2(pbt)][BF_4]$ (**1**)	6.6± 2.2
$[Cu(PPh_3)_2(bopy)][BF_4]$ (**2**)	11.6 ± 3.9
$[Cu(PPh_3)_2(dpk)][BF_4]$ (**3**)	7.6 ± 3.2
$[Cu(PPh_3)_2(dpp)][BF_4]$ (**4**)	17.7 ± 5.5
$[Cu(PPh_3)_2(2,2'\text{-bipy})][BF_4]$ (**5**)	6.7 ± 2.5
$[Cu(PPh_3)_2(dcbipy)][BF_4]$ (**6**)	13.9 ± 5.0
Cisplatin	59.0 ± 12.0

and the presence of apoptotic vesicles in cells exposed to compounds **1**, **3** and **5** relative to the vehicle control and precursor (**Figures 3A** and **3B**). These results suggest that the substitution of NCMe groups by pbt, dpk and 2,2'-bipy ligands in $[Cu(PPh_3)_2(L)]^+$ result in an increase of MCF7 apoptosis (**Figure 3B**). The similar cytotoxicity of compounds **1**, **3** and **5** (**Table 3**) agrees with the apoptosis results. However, these results do not exclude that other non-apoptotic cell death mechanisms might also occur.

Cell cycle analysis

The cytostatic potential of the compounds was inferred via propidium iodide (PI) staining after MCF7 cells synchronization and incubation for 6h, 12h and 24h in the presence of the precursor and compounds **1**, **3** and **5** at their IC_{50}. DMSO was used as vehicle control, and Doxorubicin was used as positive control of cell cycle arrest on G2/M phase[34]. While treatment of samples with doxorubicin (DOXO) resulted in cell cycle arrest after 12h incubation, a careful examination of the cell cycle progression of compounds **1** and **3** shows a slight increase of the % cells in G2/M from 12h to 24h with subsequent decrease of the % cells in S and G0/G1 phases (**Figure 4**). These results suggest that treatment of MCF7 breast adenocarcinoma cancer cells with precursor and compounds **1** and **3** result in similar a cell cycle profiles, with a delay in cell cycle progression over time and, arrest in G2/M phase. Unlike the others, compound **5** shows a high cytostatic effect, causing cell cycle arrest after 24h, where 91% of the cells are at S phase. The cytotoxic (at low micromolar range) and the cytostatic capability of these compounds, particularly of compound **5**, suggest that they can be suitable for further *in vivo* studies aiming their potential translation towards breast cancer therapy.

Experimental Section

General procedures

All starting reagents and solvents were obtained from standard chemical suppliers. All manipulations involving air-free syntheses were carried out under dinitrogen atmosphere using Schlenk techniques and the solvents used were dried by standard methods[35]. Starting materials $[Cu(NCMe)_4][BF_4]$ and $[Cu(NCMe)_2(PPh_3)_2][BF_4]$ were prepared following the methods described in the literature[36, 37]. NMR spectra were recorded on a Bruker Avance 400 spectrometer (^{1}H NMR at 400.13 MHz, ^{13}C NMR at 100.6 MHz, ^{31}P NMR at 161.97 MHz) at room temperature except when stated otherwise. Chemical shifts (δ) are reported in parts per million (ppm) using CD_3CN, $CDCl_3$ or $(CD_3)_2CO$ as solvent. ^{1}H and ^{13}C chemical shifts were measured relative to solvent peaks considering internal Me_4Si (0 ppm) and the ^{31}P NMR was externally referenced to 85% H_3PO_4. Abbreviations: s = singlet, d = doublet, t = triplet, m = multiplet, q = quartet, sept = septet, m = multiplet, c = complex, br = broad, *J* = coupling constant.

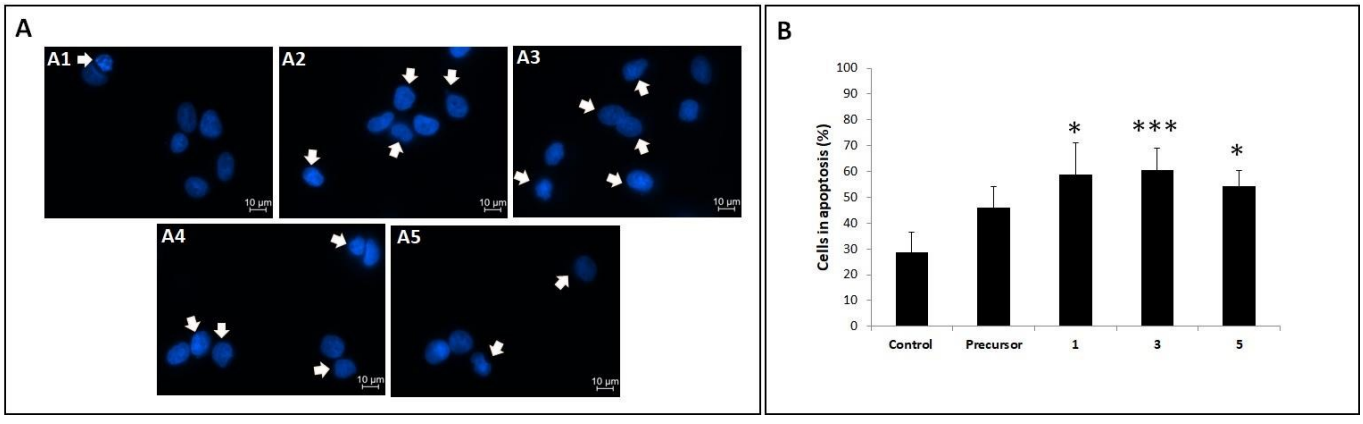

Figure 3 Morphological changes in the nucleus of MCF7 cells exposed to the precursor $[Cu(PPh_3)_2(NCMe)_2][BF_4]$ and compounds **1**, **3** and **5**. A) Nucleus of MCF7 stained with Hoechst 33258 for visualization of apoptotic events, including chromatin condensation and nucleus fragmentation (white arrows). Cells were stained after 6h treatment with culture medium (DMEM supplemented with 10 % FBS, antibiotics and non-essential amino-acids) supplemented with A1: 0.3% (v/v) DMSO (vehicle control), A2: precursor $[Cu(PPh_3)_2(NCMe)_2][BF_4]$ (at the IC_{50}), A3: compound **1** (at the IC_{50}), A4: compound **3** (at the IC_{50}), A5: compound **5** (at the IC_{50}). Images were obtained using an AXIO Scope (Carl Zeiss. Oberkochen Germany) and respective software. B) % of apoptotic MCF7 cells after 6h treatment with vehicle control, precursor and compounds **1**, **3** and **5**. Three random fields with at least 30 nuclei were selected for analysis. * p-Value < 0.05 relative to apoptosis events in MCF7 cells treated with vehicle control (DMSO). *** p-Value < 0.05 relative to apoptosis events in MCF7 treated with precursor.

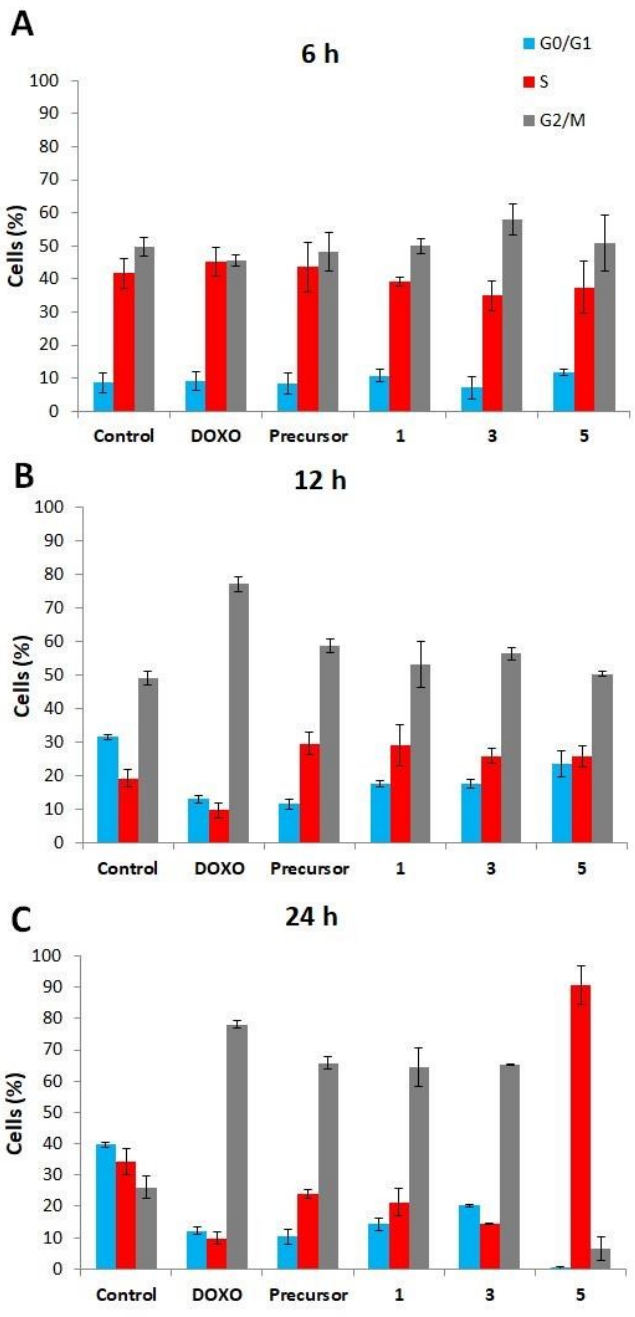

Figure 4 Cell cycle evaluation of MCF7 cells exposed to the precursor $[Cu(PPh_3)_2(NCMe)_2][BF_4]$ and compounds **1**, **3** and **5**. After two periods of synchronization at G1/S phase with thymidine, MCF7 cells were grown for A) 6 h, B) 12 h or C) 24 h in culture medium (DMEM supplemented with 10% FBS, antibiotics and non-essential amino-acids) with 0.3% (v/v) DMSO (Control), 1 μM doxorubicin (DOXO), the precursor $[Cu(PPh_3)_2(NCMe)_2][BF_4]$ (at the IC_{50}), compound **1** (at the IC_{50}), compound **3** (at the IC_{50}) or compound **5** (at the IC_{50}). The fluorescence levels of propidium iodide were determined by flow cytometry. Represented results are the mean ± SEM of three independent experiments.

2D NMR experiments (COSY, HSQC, HMBC) were used for specific assignments. Infrared spectra (4000-250 cm^{-1}) were recorded in a Thermo Nicolet 6700 spectrophotometer with KBr, only significant bands being cited in the text. Elemental analyses were obtained at our laboratories (Laboratório de Análises, at Instituto Superior Técnico), using a Fisons Instruments EA1108 system. Data acquisition, integration and handling were performed using a PC with the software package EAGER-200 (Carlo Erba Instruments). Electronic spectra (range 220-900 nm) were recorded at room temperature on a Jasco V-660 spectrometer.

Syntheses of Cu(I) complexes$[Cu(PPh_3)_2(L)][BF_4]$ (1 - 6):

General procedure

The Cu(I) complex salts **1** - **6** were prepared according to the following general synthetic procedure: the desired ligand (0.5 mmol) was added to a stirred solution of $[Cu(PPh_3)_2(NCMe)_2][BF_4]$ (0.5 mmol) in acetonitrile or THF or methanol (20 mL) and the mixture was stirred overnight at room temperature. After evaporation of the solvent under vacuum, the products were washed with n-hexane (2×10 mL) and recrystallized from dichloromethane/diethyl ether, affording crystalline products.

Data for $[Cu(PPh_3)_2(pbt)][BF_4]$ (1): solvent: THF; white crystals; yield: 85%.

^1H NMR [$CDCl_3$, 400.13 MHz] δ/ppm: 8.30 (d, 5.2 Hz, 1H, H-1), 8.13 (t, 7.6 Hz, 1H, H-3), 8.05 (d, 8.0 Hz, 1H, H-4), 7.81 (d, 6.6 Hz, 1H, H-9), 7.54 (s, 1H, H-7), 7.48 - 7.45 (m*, 1H, H-2), 7.43 (s br*, 3H, H-10, H-11, H-12), 7.40 (t, 7.5 Hz, 6H, H-*p* P*Ph*$_3$), 7.20 (t, 7.5 Hz, 12H, H-*m* P*Ph*$_3$), 7.01 (s br, 12H, H-*o* P*Ph*$_3$). $^{13}C\{^1H\}$ NMR [$CDCl_3$, 100.61 MHz] δ/ppm: 151.9 (C-5), 149.3 (C-1), 141.1 (C-8), 140.5 (C-6), 140.3 (C-3), 137.7 (C-13), 133.2 (C-*o* P*Ph*$_3$), 130.9 (C-*p* P*Ph*$_3$), 130.5 (t, $^1J_{C\text{-}P}$ =19.0 Hz, C-*ipso* P*Ph*$_3$), 129.3 (C-*m* P*Ph*$_3$), 126.8 and 126.4 (C-10 and C-11), 125.8 (C-9), 125.4 (C-7), 125.3 (C-2), 123.9 (C-4) 122.7 (C-12). $^{31}P\{^1H\}$ NMR [$CDCl_3$ 161.97 MHz] δ/ppm: 1.1 (br). FT-IR[KBr, cm^{-1}]: 3100-3040 cm^{-1} ($\nu_{C\text{-}H}$, phenyl rings), 1590-1450 cm^{-1} ($\nu_{C=N}$, $\nu_{C=C}$, phenyl rings), 1057 and 690 cm^{-1} ($\nu_{B\text{-}F}$, BF4), 700-690 cm^{-1} ($\delta_{C\text{-}H}$, phenyl rings). Elemental analysis (%) found: C, 66.5; H, 4.5; N, 1.5; S, 4.0; Calc. for $C_{49}CuH_{39}NSP_2BF_4$ (886.20): C, 66.41; H, 4.44; N, 1.58; S, 3.62. * Partial overlap

Data for $[Cu(PPh_3)_2(bopy)][BF_4]$ (2): solvent: THF; red crystals; yield:89%.

^1H NMR [$CDCl_3$, 400.13 MHz] δ/ppm: 8.56 (d, 4.8 Hz, 1H, H-1), 8.30 (t, 7.6 Hz, 1H, H-3), 8.12 (d, 7.8 Hz, 1H, H-4), 7.88 – 7.85 (m, 1H, H-2), 7.69 (t, 7.3 Hz, 1H, H-10), 7.62 (d, 7.7 Hz, 2H, H-8 and H-12), 7.54 (t, 7.8 Hz, 2H, H-9 and H-11), 7.38 (t, 7.3 Hz, 6H, H-*p* P*Ph*$_3$), 7.23 (t, 7.6 Hz, 12H, H-*m* P*Ph*$_3$), 7.15 (s br, 12H, H-*o* P*Ph*$_3$). $^{13}C\{^1H\}$ NMR [$CDCl_3$, 100.61 MHz] δ/ppm: 195.3 (C-6), 150.7 (C-1), 148.2 (C-5), 139.9 (C-3), 134.6 (C-7), 134.4 (C-10), 133.3 (t, $^2J_{C\text{-}P}$ =6.1 Hz, C-*o* P*Ph*$_3$), 131.1 (t, $^1J_{C\text{-}P}$ =17.4 Hz, C-*ipso* P*Ph*$_3$), 130.7 (C-*p* P*Ph*$_3$ + C-2 + C-4), 130.3 (C-8 + C-12), 129.2 (br, C-*m* P*Ph*$_3$), 129.1 (C-9 + C-11). $^{31}P\{^1H\}$ NMR [$CDCl_3$ 161.97 MHz] δ/ppm: 1.8 (br). FT-IR [KBr, cm^{-1}]: 1626 cm^{-1} ($\nu_{C=O}$), 3100-3040 cm^{-1} ($\nu_{C\text{-}H}$, phenyl rings), 1500-1420 cm^{-1} ($\nu_{C=N}$, $\nu_{C=C}$, phenyl rings), 1094 and 699 cm^{-1} ($\nu_{B\text{-}F}$, BF_4), 700-690 cm^{-1} ($\delta_{C\text{-}H}$, phenyl rings). Elemental analysis (%) found: C, 66.9; H, 4.6; N, 1.6; Calc. for $C_{48}CuH_{39}NOP_2BF_4$ (858.13): C, 67.18; H, 4.58; N, 1.63.

Data for $[Cu(PPh_3)_2(dpk)][BF_4]$ (3): solvent: THF; brown crystals; yield: 82%.

^{1}H NMR [$(CD_3)_2CO$, 400.13 MHz] δ/ppm: 8.65 (d, 4.6 Hz, 2H, H-1), 8.52 (d, 8.0 Hz, 2H, H-4), 8.22 (td, 7.8 and 1.4 Hz, 2H, H-3), 7.72 (m, 2H, H-2), 7.47 (t, 7.4 Hz, 6H, H-*p* PPh_3), 7.33 (t, 7.5 Hz, 12H, H-*m* PPh_3), 7.25 (t, 8.5 Hz, 12H, H-*o* PPh_3). ^{13}C{^{1}H} NMR [$(CD_3)_2CO$, 100.61 MHz] δ/ppm: 189.1 C-6), 153.0 (C-5), 151.0 (C-1), 139.9 (C-3), 134.1 (d, $^2J_{C-P}$ =14.1 Hz, C-*o* PPh_3), 132.4 (d, $^1J_{C-P}$ =31.8 Hz, C-*ipso* PPh_3), 131.4 (C-*p* PPh_3), 130.0 (d, $^3J_{C-P}$ =8.6 Hz, C-*m* PPh_3), 129.8 (C-2), 129.5 (C-4). ^{31}P{^{1}H} NMR [$(CD_3)_2CO$, 161.97 MHz] δ/ppm: 1.0 (br). FT-IR [KBr, cm^{-1}]: 1667 cm^{-1} ($\nu_{C=O}$), 3100-3040 cm^{-1} (ν_{C-H}, phenyl rings), 1500-1400 cm^{-1} ($\nu_{C=C}$, phenyl rings), 1312 cm^{-1} ($\nu_{C=N}$), 1058 and 698 cm^{-1} (ν_{B-F}, BF_4), 700-690 cm^{-1} (δ_{C-H}, phenyl rings). Elemental analysis (%) found: C, 65.5; H, 4.6; N, 2.9; Calc. for $C_{47}CuH_{38}N_2OP_2BF_4$ (859.11): C, 65.71; H, 4.46; N, 3.26.

Data for $[Cu(PPh_3)_2(dpp)][BF_4]$ (4): solvent: THF; yellow crystals; yield: 91%.

^{1}H NMR [$(CD_3)_2CO$, 400.13 MHz], T= -50 °C, δ/ppm: 8.89 (d, 4.8 Hz, 1H, H-1), 8.76 (s br, 1H, H-7), 8.68 (d, 2.3 Hz, 1H, H-8), 8.53 (d, 4.0 Hz, 1H, H-14), 8.23 (s br, 2H, H-11 and H-12), 7.85 (t, 7.8 Hz, 1H, H-3), 7.68 – 7.65 (m, 1H, H-13), 7.46 – 7.40 (c, 7H, H-2 and H-*p* PPh_3), 7.38 (d, 8.1 Hz, 1H, H-4), 7.30 (t, 7.5 Hz, 12H, H-*m* PPh_3), 7.19 – 7.15 (m, 12H, , H-*o* PPh_3). ^{13}C NMR [$(CD_3)_2CO$, 100.61 MHz], T= -50 °C, δ/ppm: 156.5 (C-10), 155.0 (C-9), 152.7 (C-5), 150.8 (C-1), 150.1 (C-14), 147.6 (C-6), 145.2 (C-8), 142.5 (C-7), 139.0 (C-12), 137.9 (C-3), 133.7 (t, $^2J_{C-P}$ =7.6 Hz, C-*o* PPh_3), 132.5 (t, $^1J_{C-P}$ = 17.4 Hz, C-*ipso* PPh_3), 131.1 (C-*p* PPh_3), 129.7 (t, $^3J_{C-P}$ = 4.7 Hz, C-*m* PPh_3), 128.8 (C-4), 126.8 (C-2), 126.0 (C-13), 125.3 (C-11). ^{31}P{^{1}H} NMR [$(CD_3)_2CO$, 161.97 MHz], T= -50 °C, δ/ppm: 2.2 (br). FT-IR [KBr, cm^{-1}]: 3100-3040 cm^{-1} (ν_{C-H}, phenyl rings), 1588-1435 cm^{-1} ($\nu_{C=C}$, phenyl rings), 1398 cm^{-1} ($\nu_{C=N}$), 1095 and 690 cm^{-1} (ν_{B-F}, BF_4), 700-690 cm^{-1} (δ_{C-H}, phenyl rings). Elemental analysis (%) found: C, 61.7; H, 4.2; N, 5.5; Calc. for $C_{49}CuH_{40}N_4P_2BF_4 \cdot 0.8CH_2Cl_2$ (965.11): C, 61.98; H, 4.34; N, 5.81.

Data for $[Cu(PPh_3)_2(2,2'\text{-bipy})][BF_4]$ (5): solvent: acetonitrile; red crystals; yield: 92%.

^{1}H NMR [$(CD_3)_2CO$, 400.13 MHz] δ/ppm: 8.62 (s br, 2H, H-1), 8.62 (d br, 7.6 Hz, 2H, H-4), 8.19 (t br, 2H, H-3), 7.44 (tt, 7.4 and 7.1 Hz, 6H, H-*p* PPh_3), 7.30 (t, 7.7 Hz, 12H, H-*m* PPh_3), 7.18 (d br, 7.0 Hz, 12H, H-*o* PPh_3). ^{13}C NMR [$(CD_3)_2CO$, 100.61 MHz] δ/ppm: 152.9 (C-5), 150.9 (C-1), 140.0 (C-3), 134.0 (C-*o* PPh_3), 133.0 (br, C-*ipso* PPh_3), 131.1 (C-*p* PPh_3), 129.8 (br, C-*m* PPh_3), 127.2 (C-2), 123.9 (C-4). ^{31}P{^{1}H} NMR [$(CD_3)_2CO$, 161.97 MHz] δ/ppm: 2.1 (br). FT-IR [KBr, cm^{-1}]: 3100-3040 cm^{-1} (ν_{C-H}, phenyl rings), 1589-1435 cm^{-1} ($\nu_{C=C}$, phenyl rings), 1315 cm^{-1} ($\nu_{C=N}$), 1049 and 694 cm^{-1} (ν_{B-F}, BF_4), 700-690 cm^{-1} (δ_{C-H}, phenyl rings). Elemental analysis (%) found: C, 66.4; H, 4.5; N, 3.3; Calc. for $C_{46}CuH_{38}N_2P_2BF_4$ (831.1): C, 66.48; H, 4.61; N, 3.37.

Data for $[Cu(PPh_3)_2(dcbipy)][BF_4]$ (6): solvent: methanol; yellow crystals; yield: 87%.

^{1}H NMR [$CDCl_3$, 400.13 MHz] δ/ppm: 9.34 (s br, 2H, H-4), 8.45 (d, 5.2 Hz, 2H, H-1), 8.00 (d, 2H, H-2), 7.37 (t, 7.4 Hz, 6H, H-*p* PPh_3), 7.21 (t, 7.5 Hz, 12H, H-*m* PPh_3), 7.07 (s br, 12H, H-*o* PPh_3), 4.08 (s br, OH). ^{13}C NMR [$CDCl_3$, 100.61 MHz] δ/ppm: 165.8 (C-6), 152.3 (C-5), 150.2 (C-1), 141.1 (C-3), 133.1 (C-*o* PPh_3), 131.6 (br, C-*ipso* PPh_3), 130.7 (br, C-*p* PPh_3), 129.2 (br, C-*m* PPh_3), 126.3 (C-2), 123.4 (C-4). ^{31}P{^{1}H} NMR [$CDCl_3$, 161.97 MHz] δ/ppm: 3.1 (br). FT-IR [KBr, cm^{-1}]: 3100-3040 cm^{-1} (ν_{C-H}, phenyl rings), 1720 cm^{-1} ($\nu_{C=O}$), 1580-1430 cm^{-1} ($\nu_{C=C}$, phenyl rings), 1380 cm^{-1} ($\nu_{C=N}$), 1056 and 694 cm^{-1} (ν_{B-F}, BF_4), 700-690 cm^{-1} (δ_{C-H}, phenyl rings). Elemental analysis (%) found: C, 63.1; H, 4.1; N, 3.0; Calc. for $C_{48}CuH_{38}N_2O_4P_2BF_4$ (919.12): C, 62.72; H, 4.17; N, 3.05.

X-ray crystallography

Crystals of **1**, **2**, **3**, **4** and **5**, suitable for X-ray diffraction study were mounted on a loop with Fomblin© protective oil. X-ray diffraction data were collected on a Bruker AXS-KAPPA APEX II diffractometer with graphite-monochromated radiation (Mo Kα, λ = 0.71073 Å) at 150 K. Crystals of compound **4** had poor quality and diffracting power, resulting in a low theta full value. The X-ray generator was operated at 50 kV and 30 mA, and the X-ray data collection was monitored by the APEX2[38] program. Empirical absorption correction using SADABS[39] was applied and data reduction was done with SMART and SAINT programs[40]. Data collection and refinements details are listed in **Table 4**. SHELXS[41] were used for structure solution, and SHELXL[42] was used for full matrix least-squares refinement on F^2. Both programs are included in the package of programs WINGX-Version 2014.1[43]. Non-hydrogen atoms were refined anisotropically. All the hydrogen atoms were inserted in calculated positions and allowed to refine in the parent carbon atom. The hydrogen bonds and intermolecular interactions were calculated by PLATON[44]. The graphical representations were prepared using MERCURY 3.8[45].

Biological assays

Cell lines and culture conditions

Human MCF7 (breast) cancer cells were grown in 25 cm^2 culture flasks as adherent monolayers in complete culture medium DMEM + GlutaMax I containing 10% heat-inactivated fetal bovine serum (FBS) and 1% antibiotics. Cultures were maintained at 37°C, 5% CO_2 in a humidified atmosphere using a CO_2 incubator (Heraeus, Germany). Cell media and supplements, phosphate buffer saline (PBS) and tripsin-EDTA were obtained from Gibco, Invitrogen (Thermo Fisher Scientific, USA).

MTT assay

Cytotoxicity was measured by the MTT assay[26]. Briefly, cells were cultured until approx. 80% confluence in culture flasks and were detached by trypsin. Then 20000 cells/well were seeded into 96-well plates with culture medium and incubated for 24 h. Compounds were first solubilized in DMSO (5 mM) and then in medium through serial dilutions from 50 µM to 0.01 µM. After treatment with the compounds the cell medium was replaced by 200 µL (0.5 mg/ml) of an MTT solution (MTT = 3-(4,5-Dimethylthiazol-2-yl)-2,5-diphenyltetrazolium bromide) in PBS and further incubated for 3 h at 37 °C. The resulting formazan product were solubilized in DMSO and

absorbance measured at 575 nm. Each experiment was repeated at least twice, and each concentration tested with at least six replicates. The IC_{50} values were calculated from concentration–response curves using the GraphPad Prism software (vs. 5.0).

View Article Online
DOI: 10.1039/C8DT01653D

Table 4 Data collection and structure refinement parameters for $[Cu(PPh_3)_2(pbt)][BF_4]$ (**1**), $[Cu(PPh_3)2(bopy)][BF_4]$ (**2**), $[Cu(PPh_3)_2(dpk)][BF_4]$ (**3**), $[Cu(PPh_3)_2(dpp)][BF_4]$ (**4**) and $[Cu(PPh_3)_2(2,2'\text{-bipy})][BF_4]$ (**5**)

Compound	1	2	3	4	5
Empirical formula	$C_{49}H_{39}BCuF_4NP_2S$	$C_{48}H_{39}BCuF_4NOP_2$	$C_{47}H_{38}BCuF_4N_2OP_2$	$C_{50.86}H_{41.72}BCl_{1.72}CuF_4N_4P_2$	$C_{47}H_{40}BCl_2CuF_4N_2P_2$
Formula Weight	886.16	858.09	859.08	994.07	916.00
T (K)	160(2)	150(2)	150(2)	150(2)	150(2)
Wavelength (Å)	0.71073	0.71073	0.71073	0.71073	0.71073
Crystal System	Triclinic	Triclinic	Triclinic	Triclinic	Triclinic
Space Group	P-1	P-1	P-1	P-1	P-1
a (Å)	10.8372(5)	10.987(5)	11.1690(7)	11.952(2)	10.5640(14)
b (Å)	11.9688(6)	13.145(6)	13.8156(9)	13.949(2)	12.4697(16)
c (Å)	17.1523(7)	16.023(7)	15.0939(9)	14.710(3)	17.463(2)
α (°)	90.664(2)	96.187(19)	83.627(2)	100.285(8)	102.070(6)
β (°)	105.748(2)	94.340(19)	69.883(2)	98.437(9)	97.123(6)
γ (°)	101.455(2)	106.60(2)	71.108(2)	95.128(8)	103.401(6)
Volume ($Å^3$)	2093.57(17)	2191.0(18)	2069.2(2)	2370.1(7)	2152.0(5)
Z	2	2	2	2	2
Calculated density (Mgm^{-3})	1.406	1.301	1.379	1.393	1.414
Absorption Coefficient (mm^{-1})	0.702	0.624	0.662	0.697	0.760
F (000)	912	884	884	1020	940
θ Range for data collection (°)	3.122 to 26.425	2.450 to 25.697	2.855 to 26.765	1.494 to 25.753	1.213 to 26.201
Limiting indices	13 ≤ h ≤ 13 -14 ≤ k ≤ 14 -21 ≤ l ≤ 20	-13 ≤ h ≤ 13 -15 ≤ k ≤ 15 -19 ≤ l ≤ 19	-14 ≤ h ≤ 14 -17 ≤ k ≤14 19 ≤ l ≤ 19	-14 ≤ h ≤ 14 -17 ≤ k ≤ 17 -17 ≤ l ≤ 17	-13 ≤ h ≤ 12 -15 ≤ k ≤ 15 -20 ≤ l ≤ 21
Reflections collected/ unique	28011 / 8536 [R(int) = 0.0391]	28081 / 8005 [R(int) = 0.0356]	27745 / 8765 [R(int) = 0.0703]	29051 / 8451 [R(int) = 0.0385]	26721 / 8186 [R(int) = 0.0276]
Completeness to θ	99.7%	97.2%	99.6 %	93.8 %	95.9%
Data/ restraints/ parameters	8536 / 0 / 532	8004/ 0 / 463	8765 / 0 / 523	8451 / 31 / 542	8186 / 0 / 532
Goodness-on-fit on F^2	1.080	1.144	1.035	1.025	0.991
Final R indices [I>2σ(I)]	R1 = 0.0396, wR2 = 0.1039	R1 = 0.0670, wR2 = 0.1944	R1 = 0.0574, wR2 = 0.1362	R1 = 0.0861, wR2 = 0.2325	R1 = 0.0432, wR2 = 0.1288
R indices (all data)	R1 = 0.0482, wR2 = 0.1078	R1 = 0.1019, wR2 = 0.2119	R1 = 0.0840, wR2 = 0.1528	R1 = 0.1155, wR2 = 0.2478	R1 = 0.0571, wR2 = 0.1413
Largest diff. peak and hole $(eÅ)^{-3}$	0.906 and -0.624	1.357 and -1.058	0.790 and -0.551	2.182 and -1.176	1.605 and -0.658

Apoptosis evaluation by Hoechst 33258 labelling

MCF7 cells were plated in 24-wells plate containing a sterilized coverslip at 50,000 cells/well. Culture medium was removed 24 h after platting and replaced with 500 µL of fresh medium containing $[Cu(PPh_3)_2(NCMe)_2][BF_4]$ or derived compounds **1**, **3** or **5** at IC_{50} concentration (**Table 3**), or 0.3% (v/v) DMSO (vehicle control). After 6h incubation at 37°C, 5% (v/v) CO_2 and 99% (v/v) relative humidity, the medium was removed and cells washed twice with phosphate buffer saline (PBS). Cell DNA was then stained for 15 min at 37°C with 7.5µg/mL Hoechst 33258 (LifeTechnologies). Cells were washed 3 times with PBS, fixed for 20 min with Formaldehyde 4%, washed again 3 times with PBS, and placed on top of a glycerol drop in a microscope slide. At least five images with 30 cells were obtained and analyzed using the AxioImager D2 fluorescence microscope (Zeiss) and corresponding software. Results are represented as mean ± SEM of three independent experiments. Statistical analysis consisting in one-way ANOVA and t-test analysis, was performed using GraphPad Prism software version 6.01.

Cell cycle analysis

Cells were seeded in a 6-well plate at 200,000 cells/well and synchronized in early S-phase using a thymidine double block, as previously described[46]. After the second block, the medium was replaced with fresh medium containing each compound, 1 µM Doxorubicin (control of cell cycle arrest) or 0.3 % (v/v) DMSO (vehicle control). Cells were collected by trypsinization with Tryple Express (LifeTechnologies) after 0 h, 6 h, 12 h and 24 h incubation at 37°C, 5 % (v/v) CO_2 and 99 % (v/v) relative humidity. After a centrifugation at 650 xg for 5 min at 4 °C, pelleted cells were washed with 1 mL cold PBS and centrifuged at 3,000 *x*g for 5 min at 4 °C. Cells were then suspended in 100 µL cold PBS, submitted to an up-and-down pipetting to assure complete cell disaggregation and added drop by drop in a 1 mL cold ethanol solution 80 % (v/v). After at least 12 h incubation at 4 °C, cell suspension was centrifuged at 5,000 xg for 10 min at 4 °C, ethanol was completely removed, cells were treated for 30 min with an RNase 50 µg/mL solution at 37 °C, and propidium iodide was then added to a final concentration of 25 µg/mL. Data was collected using an Attune acoustic focusing cytometer (ThermoFisher Scientific) and analyzed using FCS express flow cytometry vs 6 (De Novo Software).

Statistical analysis

All data were expressed as mean ± SEM from at least three independent experiments. Statistical significance was evaluated using the Student's t-test; $p < 0.05$ was considered statistically significant.

Conclusions

A family of copper(I) complexes with N,N-, N,O- and N,S-bidentate heteroaromatic ligands have been synthesized and fully characterized.

All the compounds were active *in vitro* against MCF7 human breast adenocarcinoma cancer cells with IC_{50} values in the micromolar range. Interestingly, all the compounds are far more active in the breast cancer cells than the metallodrug cisplatin. The introduction of two carboxyl substituents in the 2,2'-bipy ligand resulted in a loss of activity that can be related to the double negative charge acquired by the compound in solution which could hinder the cellular uptake. Compounds 1 and 3 induces MCF7 apoptotic cell death and a cell cycle arrest in G2/M phase. Compound 5, unlike the others, showed a high cytostatic effect, causing cell cycle arrest at the S phase. The cytotoxic and cytostatic effects exhibited by these compounds suggest that additional *in vivo* studies should be performed in order to validate their potential action as anticancer agents towards breast cancer.

Conflicts of interest

There are no conflicts to declare.

Acknowledgements

View Article Online
DOI: 10.1039/C8DT01653D

We thank the Fundação para a Ciência e Tecnologia (FCT) for the financial support (UID/QUI/00100/2013 (CQE), UID/Multi/04378/2013 (UCIBIO) and UID/Multi/04349/2013 (C2TN/IST)). Unidade de Ciências Biomoleculares Aplicadas – UCIBIO also thank the co-financing by the ERDF under the PT2020 Partnership Agreement (POCI-01-0145-FEDER-007728). Tânia S. Morais thanks FCT for her post-doctoral grant (SFRH/BPD/93513/2013).

Notes and references

1. K. G. Daniel, R. H. Harbach, W. C. Guida and Q. P. Dou, *Front. Biosci.*, 2004, **9**, 2652-2662.
2. D. S. Kalinowski, C. Stefani, S. Toyokuni, T. Ganz, G. J. Anderson, N. V. Subramaniam, D. Trinder, J. K. Olynyk, A. Chua, P. J. Jansson, S. Sahni, D. J. Lane, A. M. Merlot, Z. Kovacevic, M. L. Huang, C. S. Lee and D. R. Richardson, *Biochim. Biophys. Acta*, 2016, **1863**, 727-748.
3. A. Hordyjewska, L. Popiolek and J. Kocot, *Biometals*, 2014, **27**, 611-621.
4. L. D. D'Andrea, A. Romanelli, R. Di Stasi and C. Pedone, *Dalton Trans.*, 2010, **39**, 7625-7636.
5. G. Crisponi, V. M. Nurchi, D. Fanni, C. Gerosa, S. Nemolato and G. Faa, *Coord. Chem. Rev.*, 2010, **254**, 876-889.
6. A. Gupte and R. J. Mumper, *Cancer Treat Rev*, 2009, **35**, 32-46.
7. J. Wachsmann and F. Peng, *World J. Gastroenterol.*, 2016, **22**, 221-231.
8. C. Marzano, M. Pellei, F. Tisato and C. Santini, *Anticancer Agents Med. Chem.*, 2009, **9**, 185-211.
9. S. Tardito and L. Marchio, *Curr. Med. Chem.*, 2009, **16**, 1325-1348.
10. F. Tisato, C. Marzano, M. Porchia, M. Pellei and C. Santini, *Med. Res. Rev.*, 2010, **30**, 708-749.
11. C. Santini, M. Pellei, V. Gandin, M. Porchia, F. Tisato and C. Marzano, *Chem. Rev.*, 2014, **114**, 815-862.
12. Z. Zhang, Y. Gou, J. Wang, K. Yang, J. Qi, Z. Zhou, S. Liang, H. Liang and F. Yang, *Eur. J. Med. Chem.*, 2016, **121**, 399-409.
13. N. Mukherjee, S. Podder, S. Banerjee, S. Majumdar, D. Nandi and A. R. Chakravarty, *Eur. J. Med. Chem.*, 2016, **122**, 497-509.
14. C. Marzano, M. Pellei, D. Colavito, S. Alidori, G. G. Lobbia, V. Gandin, F. Tisato and C. Santini, *J. Med. Chem.*, 2006, **49**, 7317-7324.
15. V. Gandin, M. Porchia, F. Tisato, A. Zanella, E. Severin, A. Dolmella and C. Marzano, *J. Med. Chem.*, 2013, **56**, 7416-7430.
16. M. Wehbe, A. W. Y. Leung, M. J. Abrams, C. Orvig and M. B. Bally, *Dalton Trans.*, 2017, **46**, 10758-10773.
17. W. Villarreal, L. Colina-Vegas, G. Visbal, O. Corona, R. S. Corrêa, J. Ellena, M. R. Cominetti, A. A. Batista and M. Navarro, *Inorg. Chem.*, 2017, **56**, 3781-3793.
18. D. Denoyer, S. Masaldan, S. La Fontaine and M. A. Cater, *Metallomics*, 2015, **7**, 1459-1476.
19. C. X. Zhang and S. J. Lippard, *Curr Opin Chem Biol*, 2003, **7**, 481-489.

20. T. Pivetta, V. Lallai, E. Valletta, F. Trudu, F. Isaia, D. Perra, E. Pinna and A. Pani, *J. Inorg. Biochem.*, 2015, **151**, 107-114.
21. F. R. Kona, D. Buac and M. B. A, *Curr. Cancer Drug Targets*, 2011, **11**, 338-346.
22. V. Gandin, M. Pellei, F. Tisato, M. Porchia, C. Santini and C. Marzano, *J. Cell. Mol. Med.*, 2012, **16**, 142-151.
23. A. S. Mendo, S. Figueiredo, C. Roma-Rodrigues, P. A. Videira, Z. Ma, M. Diniz, M. Larguinho, P. M. Costa, J. C. Lima, A. J. Pombeiro, P. V. Baptista and A. R. Fernandes, *J. Biol. Inorg. Chem.*, 2015, **20**, 935-948.
24. Z. Ma, B. Zhang, M. F. C. Guedes da Silva, J. Silva, A. S. Mendo, P. V. Baptista, A. R. Fernandes and A. J. L. Pombeiro, *Dalton Trans.*, 2016, **45**, 5339-5355.
25. K. Czerwinska, B. Machura, S. Kula, S. Krompiec, K. Erfurt, C. Roma-Rodrigues, A. R. Fernandes, L. S. Shul'pina, N. S. Ikonnikov and G. B. Shul'pin, *Dalton Trans.*, 2017, **46**, 9591-9604.
26. J. Lopes, D. Alves, T. S. Morais, P. J. Costa, M. F. M. Piedade, F. Marques, M. J. Villa de Brito and M. Helena Garcia, *J. Inorg. Biochem.*, 2017, **169**, 68-78.
27. S. Keller, A. Pertegas, G. Longo, L. Martinez, J. Cerda, J. M. Junquera-Hernandez, A. Prescimone, E. C. Constable, C. E. Housecroft, E. Orti and H. J. Bolink, *J. Mater. Chem.*, 2016, **4**, 3857-3871.
28. I. Andres-Tome, J. Fyson, F. Baiao Dias, A. P. Monkman, G. Iacobellis and P. Coppo, *Dalton Trans.*, 2012, **41**, 8669-8674.
29. D. E. Janzen, S. R. Doherty, D. G. VanDerveer, L. M. Hinkle, D. A. Benefield, H. M. Vashi and G. J. Grant, *J. Organomet. Chem.*, 2014, **755**, 47-57.
30. M. Navarro, O. A. Corona, T. Gonzalez and M. V. Capparelli, *Acta Crystallogr. sec E*, 2008, **64**, m533-534.
31. E. Frohlich, *Int. J. Nanomed*, 2012, **7**, 5577-5591.
32. V. Gandin, F. Tisato, A. Dolmella, M. Pellei, C. Santini, M. Giorgetti, C. Marzano and M. Porchia, *J. Med. Chem.*, 2014, **57**, 4745-4760.
33. O. Kepp, L. Galluzzi, M. Lipinski, J. Yuan and G. Kroemer, *Nat. Rev. Drug Discov.*, 2011, **10**, 221-237.
34. N. K. Verma, M. P. Purohit, D. Equbal, N. Dhiman, A. Singh, A. K. Kar, J. Shankar, S. Tehlan and S. Patnaik, *Bioconjug. Chem.*, 2016, **27**, 2605-2619.
35. D. D. Perrin, W. L. F. Amarego and D. R. Perrin, *Purification of Laboratory Chemicals*, Pergamon, New York, 2nd edn., 1980.
36. G. J. Kubas, B. Monzyk and A. L. Crumbliss, in *Inorg. Synth.*, John Wiley & Sons, Inc., 2007, DOI: 10.1002/9780470132500.ch18, pp. 90-92.
37. J. Díez, S. Falagán, P. Gamasa and J. Gimeno, *Polyhedron*, 1988, **7**, 37-42.
38. *APEX2 v2009.3-0*, Bruker AXS: Madison, WI, 2009.
39. *SABADS: Program for Empirical Absorption Correction*, University of Göttingen: Göttingen, Germany, 1996.
40. *SAINT, Area-detector Integration Software (Version 6.28A)*, Brucker AXS Inc., Madinson, WI, 2001.
41. G. Sheldrick, *Acta Crystallogr. Sec. A*, 2008, **64**, 112-122.
42. *SHELXL-97: Program for the Refinement of Crystal Structure*, University of Gottingen, Germany, 1997.
43. L. Farrugia, *J. Appl. Crystallogr.*, 1999, **32**, 837-838.
44. A. Spek, *Acta Crystallogr. sec D*, 2009, **65**, 148-155.
45. C. F. Macrae, P. R. Edgington, P. McCabe, E. Pidcock, G. P. Shields, R. Taylor, M. Towler and J. van de Streek, *J. Appl. Crystallogr.*, 2006, **39**, 453-457.
46. P. M. Borralho, B. T. Kren, R. E. Castro, I. B. Moreira da Silva, C. J. Steer and C. M. P. Rodrigues, *FEBS J.*, 2009, **276**, 6689-6700.

View Article Online
DOI: 10.1039/C8DT01653D

Table of contents

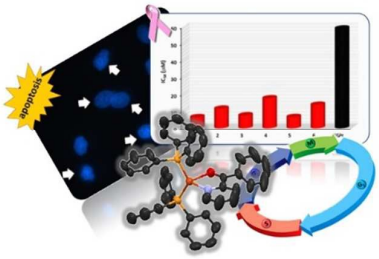

Synthesis of new phosphane-Cu(I) complexes with bidentate ligands displaying cytotoxic and cytostatic effects that make them attractive as anticancer agents.